Local Heat-Transfer Characteristics of Glaze-Ice Accretions on an NACA 0012 Airfoil

M. R. Pais,* S. N. Singh,† and L. Zou‡
University of Kentucky, Lexington, Kentucky

Laboratory-scale experiments were conducted in the subsonic wind-tunnel facility at the University of Kentucky. Experimental convective local heat-transfer coefficients were obtained for a simulated, full-scale, selected set of 0- and 5-min glaze like ice models on an NACA 0012 airfoil. A steady-state heat-flux method was employed. Local Nusselt numbers for a smooth NACA 0012 airfoil at angles of attack $\alpha = 0$, 2, 4, 6, and 8 deg, and on a 5-min smooth glaze-ice shape on the same airfoil at $\alpha = 4$ deg were also obtained. A number of experiments were performed in the Reynolds number range of 7×10^5 to 2×10^6 based on chord. At $\alpha = 2$, 4, 6, and 8 deg, the average relative increase of the Nusselt number on the suction surface with respect to the pressure surface is 21, 36, 58, and 72%, respectively. For the 5-min model, the maximum Nusselt number occurs at the tip of the horn, where it is about 51% higher than the rest of the surface, and 25% higher for the same location on the 0-min model. A comparison with published results on an NACA 65, 2-016 airfoil is also presented.

Nomenclature

A = surface area
C = chord of airfoil
D = diameter of the leading edge
h = heat-transfer coefficient
I = current
k = thermal conductivity of air
l = distance along the surface from the leading edge
Nu_c = Nusselt number, $= hC/k$
Q = heat flux
R = radius
Re_c = Reynolds number, $= \rho UC/\mu$
t = time
T = temperature
U = velocity
V = voltage
x,y = Cartesian coordinates
α = angle of attack
μ = dynamic viscosity of air
ρ = density of air
σ = standard deviation

Subscripts

w = wall
∞ = ambient

Introduction

EXTENSIVE experiments have been performed on airfoils to measure and predict static and dynamic pressure measurements,[1,2] aerodynamic lift and drag characteristics,[3] and the droplet size and trajectories.[4,5] However, very little work has been done in determining the local heat-transfer coefficient for airfoil surfaces.[6-9] Research performed earlier on aircraft lift surfaces and engine intakes has been well documented in Ref. 10. The conditions for and structure of freezing supercooled water droplets under static conditions have been studied extensively.[11-13] Ice formation under forced convective impact conditions also has been studied under varying conditions.[14,15] It is dependent on 1) ambient temperature T_∞, 2) liquid water content, 3) droplet diameter, 4) flight velocity, 5) airfoil geometry, and 6) icing time t.

The shape of the ice accretion depends on the airfoil shape, leading-edge radius, camber, and angle of attack α.[16-18] Ice accretion is dependent on the rate at which the heat of fusion may be released to the surroundings, i.e., on the ability of the flowfield to remove heat, from which we deduce that one of the significant parameters in the ice accretion process is the local convective heat-transfer coefficient. Knowledge of the thermal boundary layer and determination of the local heat-transfer coefficient at various Reynoids numbers will assist in predicting local ice growth rates.

The ice accretion process takes place through a series of concurrently occurring energy transfer mechanisms,[14,19] simply stated as 1) convective heat losses, 2) latent heat gain, 3) heat loss due to evaporation and sublimation, and 4) heat gain due to kinetic energy.

For an adiabatic wing, the energy balance of these processes must be dissipated into the ambient through convection. As a result of the speed of most aircraft, the heat-transfer process can be considered to be forced convective. A number of ice accretion experiments already have been performed on the NACA 0012 airfoil to determine its aerodynamic characteristics.[1,16,18] It was decided to select this profile, which is commonly used on helicopters, because of its appropriateness to the problem, since such aircraft are most susceptible to icing as they are required to fly at lower altitudes below the cloud cover. Second, the determination of the local heat-transfer coefficient would complete the data bank available for both the fluid and thermal fields of this airfoil. Two models were selected for the present study: an NACA 0012 airfoil with no icing, and a 5-min glaze-ice accretion on the same airfoil at $\alpha = 4$ deg.

Received March 28, 1988; revision received July 6, 1988. This paper is declared a work of the U.S. Government and is not subject to copyright protection in the United States.

*Graduate Research Assistant; Department of Mechanical Engineering. Student Member AIAA.
†Professor, Department of Mechanical Engineering.
‡Visiting Scholar, Jiaotong University, China.

Experimental Method

The Steady-State Heat Flux Method

Newton's Law of Cooling,[20]

$$Q = hA(T_w - T_\infty) \tag{1}$$

defines the convective heat flux between a fluid at T_∞ in contact with A at T_w. It depends on the conditions within the boundary layer, which are a function of the surface geometry, the nature of the fluid motion and fluid thermodynamic and transport properties.[20,21] In applying this law to our problem of glaze-ice accretion, a case in which we have mass transfer of water from the fluid to the body surface by freezing due to convective heat loss, we can assume an isothermal surface at a temperature equal to that of the freezing point of water. Lack of experimental facilities limit an exact simulation with respect to mass transfer of water droplets from air to surface, which are assumed to be insufficiently numerious to perturb the flow. As ice accumulation builds on the leading edge of an airfoil, the flowfield must slowly adjust to the new boundary conditions imposed by the change in shape. This change in the airfoil shape, and the resulting change in the flowfield, will also alter impingement rates on the surface. Thus, the ice accretion process is also a function of time and must be modeled accordingly. One method of modeling the effect of time is a time-stepping approach, assuming ice accretion can be broken down into a series of steady-state processes. Hence, if we consider the glaze-ice at any instant in time, and assume no further ice accretion, then the geometry is fixed. The heat transfer coefficient can then be acquired experimentally as long as one can reproduce the geometry and flow conditions (Reynolds and Prandtl number), and provide an isothermal surface to ensure a similar thermal boundary layer. If the aforementioned conditions are satisfied, the heat-transfer coefficient can be evaluated from knowledge of the local heat flux and respective temperatures required by Newton's law of cooling.

Apparatus

The experiment was conducted in the subsonic wind-tunnel facility in the Department of Mechanical Engineering at the University of Kentucky. The induced-flow wind tunnel is equipped with a 50-kW axial fan and has a 4.8-mm honeycomb, 102 mm in depth, for straightening the flow, at the upstream end of the plenum chamber. The 508 × 711 × 1220-mm test section has three sides made of Plexiglass for use in flow visualization with ports provided in the sides for taking velocity measurements using a hot-film probe over a three-dimensional grid. Velocities up to 160 mph normally can be obtained in this section.

Since ice accretion is predominantly a leading-edge phenomenon, heat-transfer measurements were performed only on a section of the leading edge. The airfoil is constructed of steel-aluminum laminate. This being a good conductor of heat, it requires that a section be cut off and replaced with an insulating piece (balsa wood) of the same profile (see Fig. 1). The heaters and thermocouples were mounted on this wooden section, consistent with fabrication methods described earlier.[22] In these experiments, the problem of maintaining a uniform temperature on the surface is solved by using 20 independent narrow strips of Minco thermofoil heaters, 5.9 × 175 × 0.3 mm, glued on, with the long sides touching, to the surface of the wooden body insert of the model (see Fig. 1). The temperature of the surface is measured using thermocouples. Hence, if the model is made of insulating material, most of the heat must be dissipated directly into the fluid medium.

Each heater has an individual ac power supply. The voltage across each heater is measured using an HP3455A digital voltmeter. The current through each heater is measured by a FLUKE 8600A digital multimeter. A bank of quick disconnects makes it possible to connect the one ammeter in series

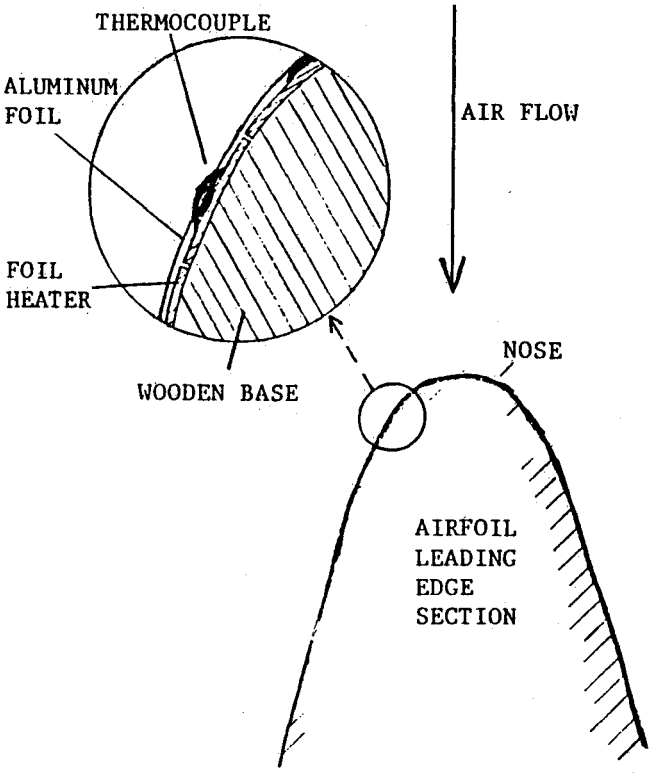

Fig. 1 Heater and thermocouple layout.

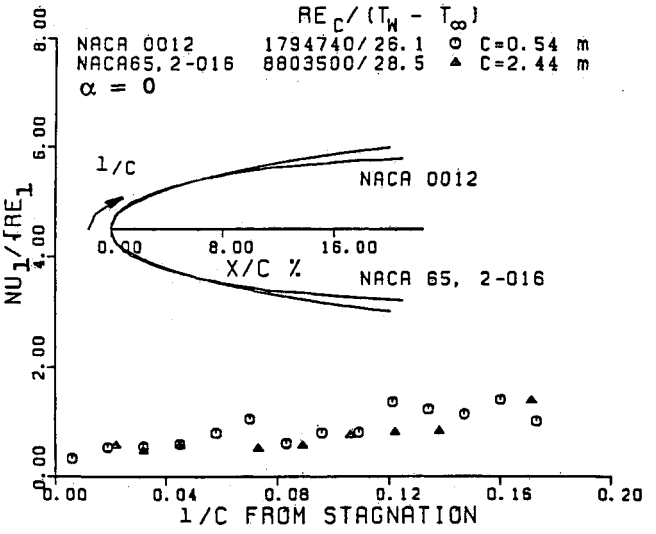

Fig. 2 Comparison of Nusselt number at $t = 0$, $\alpha = 0$ deg.

with any heater circuit, one at a time. Each heater has a 0.02-mm inconel element, which has a negligible temperature coefficient of resistance in the temperature range of interest. The heaters cover 5% of the chord on one face of the leading edge and 20% of the chord on the other face of the leading edge. In order to obtain data at various angles of attack for both the pressure and suction surfaces, the experiments had to be performed twice for the same Reynolds number with the heated section first in the suction region and then aligned so as to be in the pressure region of the flow. The chord for the NACA 0012 airfoil is $C = 536$ mm. The l/C from stagnation is the dimensionless length along the surface from the point of forward stagnation at $\alpha = 0$ deg. The wing spanned the full height of the test section and was mounted such that its angle of attack could be varied through a wide range. For all cases in

this study, the Nusselt and Reynolds numbers were calculated using the film temperature $(T_w + T_\infty)/2$ and a characteristic length, the chord C.

The temperature of each individual heater is monitored using three OMEGA copper-constantan thermocouples (0.2-mm flattened bead junction) placed equidistantly along the length. This provides not only a temperature distribution on the surface but also acts as a backup feature in case any one thermocouple malfunctions. This latter precaution is necessary since the temperature of the entire surface has to be maintained in an isothermal state within experimental limits. The thermocouple junctions are affixed to the top of the heater surface using a highly conductive Omega 101 epoxy as a heat sink. Thermocouples are also placed at the junction of the wooden ice profile with the airfoil in order to measure the base temperature from which an estimate of the conductive heat losses through the wooden model can be calculated. Less than 1% of the heat generated at the surface was conducted away from the surface. The whole assembly is finally covered with adhesive-backed, thin (0.07-mm) aluminum foil to give a smooth and continuous surface. Because the foil is thin, it is assumed that it does not affect the heat transfer into the airstream. Also, the low emissivity of aluminum reduces heat losses due to radiation (less than 0.4%). Details of the radiation and conduction corrections are given in Ref. 23. Calibrated Omega electronic ice points are used in conjunction with the thermocouples, and these voltages are read and recorded using an HP3467A logging multimeter. Electrical access to any heater or thermocouple is facilitated through a bank of scanners. The freestream temperature T_∞ is measured by a separate thermocouple mounted inside the test section. The velocity is measured using a TSI 1210-20 single hot-film sensor controlled by a TSI 1050 series constant-temperature anemometer. The linearized signal is measured by an HP3455a digital voltmeter and a DISA 55D35 rms voltmeter provides the turbulence intensity.

Experimental Procedure

The wind tunnel was allowed to run 5–10 min to attain steady flow and temperature conditions. The velocity was set so as to obtain a predetermined Reynolds number. The power to the individually controlled heaters was switched on and the thermocouple temperatures were monitored continuously until a constant temperature was attained over the surface. Once steady-state conditions were reached, the voltage across, the current through, and the thermocouple voltages on each heater were noted. Finally, the freestream temperature and velocity were recorded. The surface is heated to a predetermined temperature profile with the aid of a number of Minco thermofoil heaters. The electrical energy input is converted into thermal energy in the resistance of the heaters. After making conduction and radiation loss corrections, the convective heat flux at steady state is given by

$$Q = V \times I - \text{losses}_{(\text{radiation, conduction})} \tag{2}$$

Discussion of Results

0-Min Glaze Ice on an NACA 0012 Airfoil

A comparison of the local Nusselt number based on l with published results[7] is presented in Fig. 2 for the case of $\alpha = 0$ deg and $t = 0$. The NACA 65, 2-016 is of similar geometry[24] to the NACA 0012 airfoil in the leading-edge region. The results agree well for $l/C \leq 5\%$. Further downstream, the Nusselt number differs by up to a maximum of 50% (relative to the present data), occurring at $l/C = 7\%$. Most of the ice accretion is observed to occur within $l/C \leq 6\%$.

Figure 3 is a plot of the Nusselt number (based on chord) variation with l/C, at $\alpha = 0$ to 8 deg, for the airfoil without ice accretion. The preceding experiments were performed in the Reynolds number range of 7×10^5 to 2×10^6 based on chord, at temperature differences of approximately $(T_w - T_\infty) \approx 30°$ C. Given any angle of attack, experimental data in the form of $Nu_c/\sqrt{Re_c}$ are reproducible with a standard deviation of 4% within the tested range of Reynolds numbers, the radiation losses not being greater than 0.3% and the turbulent intensity being less than 1% in the freestream. The measurement of angle of attack was with a resolution of ± 0.5 deg. When compared to $\alpha = 0$ deg, there is an increase in the average heat transfer over the forward 18% of the chord surface region by up to 20% for $\alpha = 2$ deg. $\alpha = 4$ deg also shows an increase in the overall average heat flux over 18% of the chord by up to 14%. At $\alpha = 6$ deg, there is a 25% increase over 18% of the chord; for $\alpha = 8$ deg, a 27% increase over the same region is noted. The higher values are registered as is expected on the suction face $(l/C = -ve)$. From Fig. 3, as the angle α increases, the Nusselt number on the suction surface increases, but decreases at any location on the pressure surface $(l/C = +ve)$; a far greater increase is observed on the suction surface. At $\alpha = 2$, 4, 6, and 8 deg, the average relative increase of the Nusselt number on the suction surface with respect to the pressure surface is 21, 36, 58, and 72%, respectively, an approximately linear increase with angle of attack. The section of the airfoil normally subtended to the flow, the pressure surface, is predominantly subjected to the supercooled water droplet impingement. Icing on this face is heavier but spread out evenly over the impingement region compared to the suction surface, where, even though water impingement may be

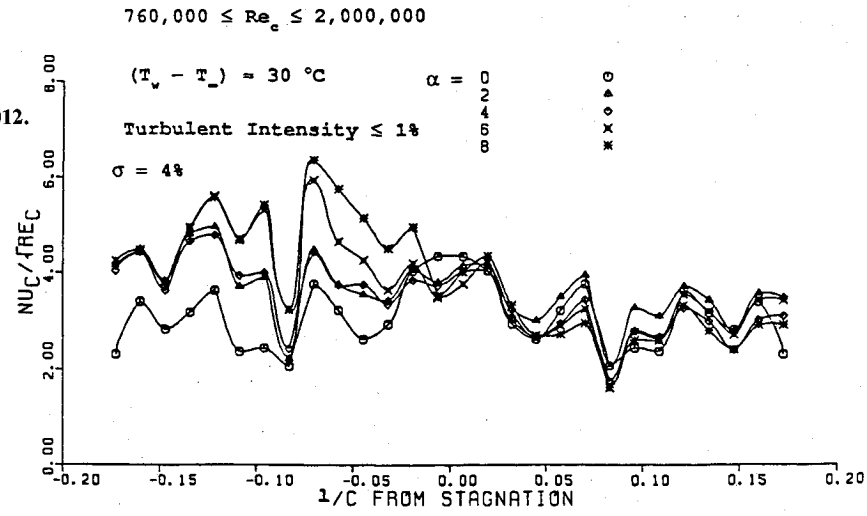

Fig. 3 Local Nusselt number on a 0-min NACA 0012.

lower because of the higher heat-flux rates, the suction surface eventually will yield a thicker ice accretion, this horn acting as a spoiler and causing premature failure of the flow around the airfoil. The coordinates of the instrumented NACA 0012 airfoil at $t=0$ are provided in Ref. 23. The profile is shown in comparison to the theoretical profile (coordinates available in Ref. 24) in Fig. 4. Surface coordinates were obtained by mounting the model on a vertical semiuniversal milling machine with a three-degree-of-freedom motion table. Using a Mititoyo digital indicator with a resolution of 0.0005 in. and a fine needle-point probe, the profile was measured over a variable grid spacing so as to get at least 10 coordinates pairs per heater element imbedded on the surface. The heater-imbedded surface does follow the contours of the theoretical profile; however, the thermocouple affixed to the top of the heater elements forms small, three-dimensional nodes on the surface not more than a millimeter in height. The wavy trend of the Nusselt number is probably due to the small surface departure in the thermocouple regions, the boundary-layer thickness in this region being of the same order of magnitude.

Within the leading-edge region of the airfoil, on the pressure surface, the data for all angles of attack tested coalesce (see Fig. 3). Consider a cylinder in crossflow. As a result of its axisymmetric geometry, no angle of attack can be ascribed to any particular axially rotated position. A similar geometric situation can be envisaged at the leading edge of the airfoil, which can be assumed to be a cylinder 26 mm in diameter. (This dimension was determined by fitting a radius gage on the leading edge of the instrumented model.) If the Nusselt number for the airfoil is calculated based on this diameter and compared with that of the stagnation region of a cylinder, the results match well up to $l/D<0.7$ (see Fig. 4). Beyond this point, the Nusselt number increases. In the preceding comparison—the calculations performed by Frossling,[25]—on a cylinder, the laminar flow conditions assumed exist for $l/D<0.7$,[26,27] beyond which the flow becomes turbulent and the Nusselt number increases. The geometry beyond $l/D<0.7$ not being similar, no more comparison is applicable.

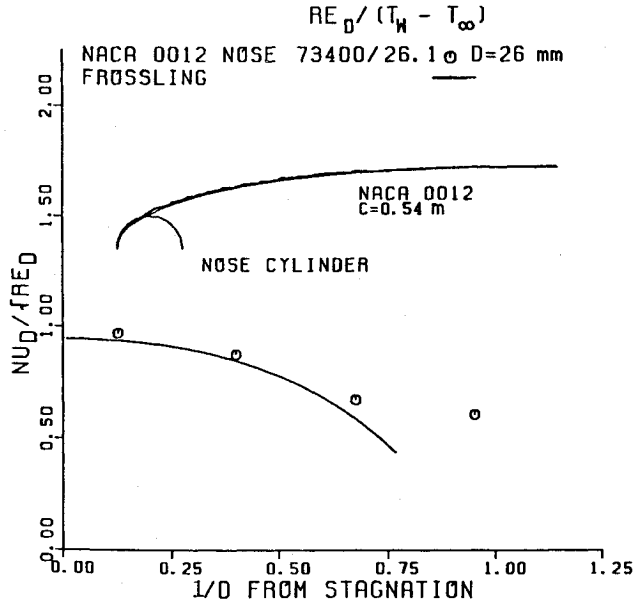

Fig. 4 Local Nusselt number on the nose of an NACA 0012.

5-Min Glaze Ice on an NACA 0012 at $\alpha=4$ deg

Further studies were also performed on a 5-min simulated glaze-ice model on an NACA 0012, coordinates for which are given in Ref. 23. Coordinates of the ice shape were determined by calculating the mean profile of an experimentally obtained ice accretion,[18] under conditions of liquid water content of 2.1 g/m^3, volume median drop size of 20 μm, and airspeed of 209 kmph on an airfoil of 0.53 m chord. Figure 5 shows the forward section of the NACA 0012 airfoil with the 5-min smooth glaze-ice shape attached. Note that this experiment was performed at $\alpha=4$ deg. The surface of the 5-min glaze-ice model was heated using 13 independent Minco heaters $5.9\times140\times0.3$ mm. The heaters cover the total projecting surface of the 5-min ice shape in the forward stagnation region of the airfoil. Figure 5 illustrates the Nusselt number variation along the surface of this model with time, for $t=0$ and 5 min of icing, at the same angle of attack. When the Nusselt number is defined using chord, it is observed that a predominant peak occurs at $l/C=-3.2\%$ of the chord along the suction surface, corresponding to the horn on the upper surface (thermocouple 2), and then levels off for the rest of the surface. Here the heat-transfer rate has increased by 26% when compared to the same location at $t=0$. In the region surrounding the horn, $-5\le l/C\le2$ (thermocouples 7, 6, 5, 1, 2, 3, 4), which constitutes the suction region, the heat-transfer rate has decreased by almost 25% of its original value at $t=0$. This suggests that the horn, at thermocouple 2, has a heat-transfer rate approximately 51% higher than its surrounding surface and, consequently, should grow outward at 1.5 times the surrounding rate. On the pressure surface (thermocouples 8, 9, 10), a marginal increase of 5% is noted. Studies performed[6,7] show that the impingement rate on this airfoil at $\alpha=0$ deg is uniform (surface is wet with no dry spots) for $l/C\le3\%$ and

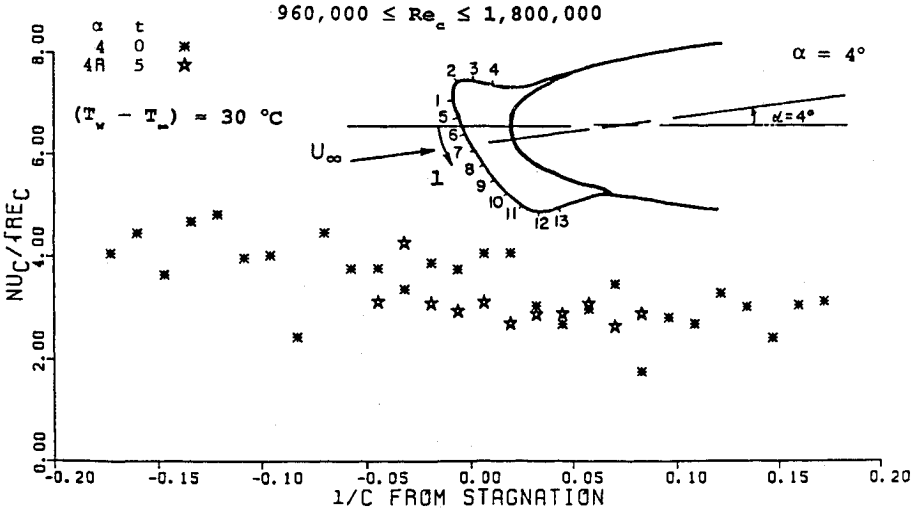

Fig. 5 Local Nusselt number on a 0- and 5-min glaze ice.

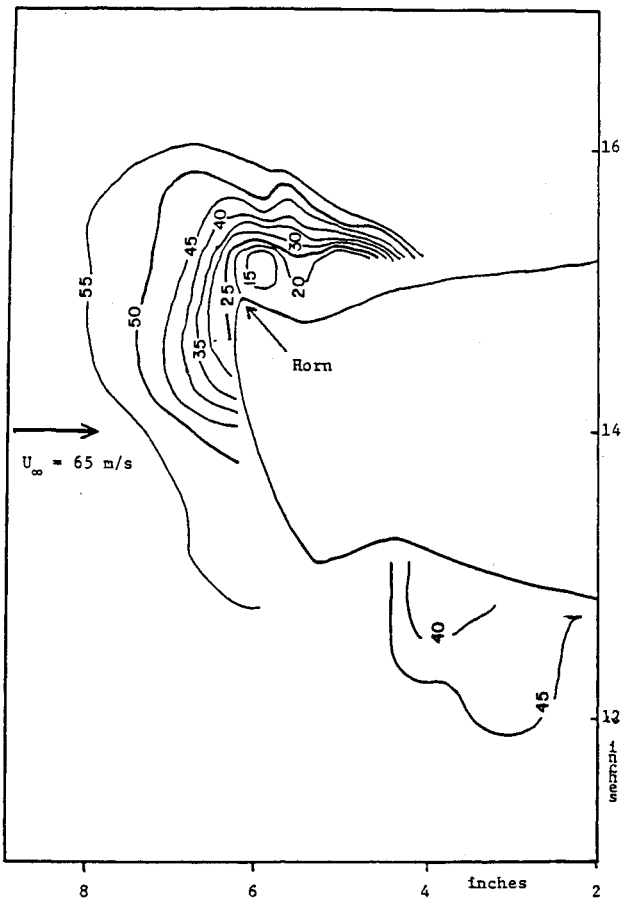

Fig. 6 Velocity field around 5-min Glaze ice.

decreases thereafter until $l/C \leq 32\%$, after which no more direct impingement takes place. Therefore, even though the capability of high heat-flux rates do exist downstream, the dearth of liquid flowing in this region precludes any ice buildup. Ice accretion studies on cylinders[22,28,29] demonstrate clearly that regions of high heat transfer correspond to the tips of the horn and maximum profile thickness. Measurements of the ice thickness at various locations of the present $t = 5$-min model show that the upper-surface horn is ≈ 1.4 times the thickness at any other location. Experiments were performed in the Reynolds number range of 9.6×10^5 to 1.8×10^6 based on chord, at temperature differences of approximately $(T_w - T_\infty) \approx 30°$ C. Given any angle of attack, experimental data in the form of $Nu_c/\sqrt{Re_c}$ are reporducible with a standard deviation of 7% within the tested range of Reynolds numbers, the radiation losses not being greater than 0.4%, and the turbulent intensity being less than 1% within the freestream. The measurement of angle of attack is within ± 0.5 deg.

Figure 6 is a contour plot of time-averaged flow speeds around this model. Time-averaged velocities were obtained using a hot-film probe over a three-dimensional grid at 12-mm intervals within a 130-mm vicinity of the leading edge. This shows a stagnation region and separated flow after the suction surface horn. This separation may be the cause of the drop in the Nusselt number at thermocouple 3, as is observed in Fig. 5.

Conclusions

The technique described herein to measure the heat-transfer coefficient gave good, reproducible results. The ice shape models were prepared meticulously, with precautions taken to conform to the initial profile as closely as possible.

Local Nusselt numbers were obtained for an NACA 0012 airfoil at various angles of attack. The suction surfaces show the higher values with increasing α. The forward stagnation region, or nose of the airfoil, shows similar results to that of a cylinder. When data from the $t = 5$-min glaze ice are compared to that at $t = 0$ min, a 51% increase in the heat-transfer coefficient is observed in the horn region of the model, this being corroborated by a 40% difference in the ice thickness in this region, showing that ice growth is strongly dependent on the local heat-flux rates. Comparisons with published results shows good agreement.

Acknowledgments

The authors would like to acknowledge the financial support given by the Air Force Systems Command and the Computational Aerodynamics Group, at the Flight Dynamics Laboratory, Wright-Patterson Air Force Base, Dayton, OH. They would like to thank Drs. Wilbur Hankey, Wladimiro Calarese, and Joe Shang for their several suggestions and helpful discussions. Thanks are also due to T. O'Canna and E. B. Yates for the preparation of the models.

References

[1]McDevitt, J. B. and Okuno, A. F., "Static and Dynamic Pressure Measurements on a NACA 0012 Airfoil in the Ames High Reynold's Number Facility," NASA-TP-2485.

[2]Bragg, M., "Experimental Flowfield Measurements," Airfoil Performance in Icing Workshop, NASA Lewis, 1985.

[3]Laschka, B. and Jesse, R. E., "Ice Accretion and Its Effects on Aerodynamics of Unprotected Aircraft Components," AGARD-AR-127, Sec. 4, 1977.

[4]Kleuters, W. and Wolfer, G., "Some Recent Results on Icing Parameters," AGARD-AR-127, 1977.

[5]Bragg, M. B., Gregorek, G. M., and Shaw, R. J., "An Analytical Approach to Airfoil Icing," AIAA Paper 81-0403, 1981.

[6]Neel, C. B., Jr., Bergrun, N. R., Jukoff, D., and Schlaff, B. A., "The Calculation of the Heat Required for Wing Thermal Ice Prevention in Specified Icing Conditions," NACA TN-1472, 1947.

[7]Gelder, T. F. and Lewis, J. P., "Comparison of Heat Transfer from Airfoil in Natural and Simulated Icing Conditions," NACA TN-2480, 1951.

[8]Frick, C. W., Jr. and McCullough, G. B., "A Method for Determining the Rate of Heat Transfer from a Wing or Streamline Body," NACA TR-830, 1945.

[9]Hardy, J. K., "Analysis of the Dissipation of Heat in Conditions of Icing from a Section of the Wing of the C-46 Airplane," NACA TR-831, 1945.

[10]"Selected Bibliography of NACA-NASA Aircraft Icing Publications," NASA TM-81651, 1981.

[11]Brownscombe, J. L. and Hallett, J., "Experimental and Field Studies of Precipitation Particles Formed by the Freezing of Supercooled Water," *Quarterly Journal of the Meteorological Society*, Vol. 93, 1967, pp. 455-473.

[12]Mason, B. J., "The Nucleation of Supercooled Water Clouds," *Science in Progress*, Vol. 44, 1956, pp. 479-499.

[13]Gray, D. M. and Male, D. H., *Editors: Handbook of Snow, Principles, Processes, Management, and Use*, Pergamon, 1981.

[14]Kleuters, W. and Wolfer, G., "Some Recent Results on Icing Parameters," AGARD-AR-127, 1977.

[15]Hankey, W. L. and Kirchner, R., "Ice Accretion of Wing Leading Edges," AFFOL-TM-79-85-FXM, June 1979.

[16]Wilder, R. W., "A Theoretical and Experimental Means to Predict Ice Accretion Shapes for Evaluation of Aircraft Handling and Performance Characteristics," AGARD-AR-127, Sec. 5, 1977.

[17]Shaw, R.J., Sotos, R.G., and Solano, F.R., "An Experimental Study of Airfoil Icing Characteristics," NASA TM-82790, 1982.

[18]Olsen, W., Shaw, R., and Newton, J., "Ice Shapes and the Resulting Drag Increase for a NACA 0012 Airfoil," NASA TN-83556, 1984.

[19]Messinger, B. L., "Analysis of an Unheated Icing Surface," *Journal of the Aeronautical Sciences*, Vol. 20, 1953, p. 29.

[20]Incropera, F. P. and DeWitt, D. P., *Fundamentals of Heat Transfer*, Wiley, New York, 1981, pp. 340-350.

[21]Kays, W. M. and Crawford M. E., *Convective Heat and Mass Transfer*, 2nd ed., McGrww-Hill, 1980, pp. 139-158.

[22]Pais, M. and Singh, S. N., "Local Heat-Transfer Coefficients of Simulated Smooth Glaze Ice Formations on a Cylinder," *Journal of Thermophysics and Heat Transfer,* Vol. 1, No. 2, April 1987.

[23]Pais, M.R., "Determination of the Local Heat-Transfer Characteristics on Glaze-Ice Accretions on a Cylinder and NACA 0012 Airfoil," Ph.D. Dissertation, Univ. of Kentucky, Lexington, KY, 1987.

[24]Abbott, I. H. and von Doenhoff, A. E., *Theory of Wing Sections,* 1st ed., McGraw-Hill, 1949.

[25]Frossling, N., "Evaporation, Heat Transfer, and Velocity Distributions in Two-Dimensional and Rotationally Symmetrical Laminar Boundary-Layer Flow," NACA TM-1432, 1958.

[26]Schmidt, E. and Wenner, K., "Warmeabgabe Uber den Umfang eines Angeblasenen Geheizten Zylinders," *Forschg. Ing.-Wes,* Vol. 12, 1941, pp. 65–73.

[27]Schlichting, H., *Boundary Layer Theory,* 6th ed., McGraw-Hill, p. 298.

[28]Arimilli, R. V. and Keshok, E. G., "Measurements of Local Convective Heat Transfer Coefficients on Ice Accretion Shapes," AIAA Paper 84-0018, 1984.

[29]Van Fossen, G. J., Simoneau, R. J., Olsen, W. A., Jr. and Shaw, R. J., "Heat Transfer Distributions Around Nominal Ice Accretion Shapes Formed on a Cylinder in the NASA Lewis Icing Research Tunnel," NASA TM-83557, 1984.

U.S. Postal Service

STATEMENT OF OWNERSHIP, MANAGEMENT AND CIRCULATION

Required by 39 U.S.C. 3685)

1A. Title of Publication	1B. PUBLICATION NO.	2. Date of Filing
Journal of Aircraft	2 7 8 0 8 0	10/25/88
3. Frequency of Issue	**3A. No. of Issues Published Annually**	**3B. Annual Subscription Price**
Monthly	12	$26.00

4. Complete Mailing Address of Known Office of Publication *(Street, City, County, State and ZIP+4 Code) (Not printers)*
370 L'Enfant Promenade, S. W.
Washington, D. C. 20024

5. Complete Mailing Address of the Headquarters of General Business Offices of the Publisher *(Not printer)*
same as above

6. Full Names and Complete Mailing Address of Publisher, Editor, and Managing Editor *(This item MUST NOT be blank)*

Publisher *(Name and Complete Mailing Address)*
American Institute of Aeronautics and Astronautics, Inc.
(same as above)

Editor *(Name and Complete Mailing Address)*
Thomas M. Weeks
(Same as above)

Managing Editor *(Name and Complete Mailing Address)*
William F. O'Connor
(same as above)

7. Owner *(If owned by a corporation, its name and address must be stated and also immediately thereunder the names and addresses of stockholders owning or holding 1 percent or more of total amount of stock. If not owned by a corporation, the names and addresses of the individual owners must be given. If owned by a partnership or other unincorporated firm, its name and address, as well as that of each individual must be given. If the publication is published by a nonprofit organization, its name and address must be stated.) (Item must be completed.)*

Full Name	Complete Mailing Address
American Institute of Aeronautics and Astronautics, Inc.	same as above

8. Known Bondholders, Mortgagees, and Other Security Holders Owning or Holding 1 Percent or More of Total Amount of Bonds, Mortgages or Other Securities *(If there are none, so state)*

Full Name	Complete Mailing Address
none	

9. For Completion by Nonprofit Organizations Authorized To Mail at Special Rates *(DMM Section 423.12 only)*
The purpose, function, and nonprofit status of this organization and the exempt status for Federal income tax purposes *(Check one)*

(1) ☒ Has Not Changed During Preceding 12 Months
(2) ☐ Has Changed During Preceding 12 Months *(If changed, publisher must submit explanation of change with this statement.)*

10. Extent and Nature of Circulation *(See instructions on reverse side)*	Average No. Copies Each Issue During Preceding 12 Months	Actual No. Copies of Single Issue Published Nearest to Filing Date
A. Total No. Copies *(Net Press Run)*	3750	3900
B. Paid and/or Requested Circulation 1. Sales through dealers and carriers, street vendors and counter sales	---	---
2. Mail Subscription *(Paid and/or requested)*	3319	3531
C. Total Paid and/or Requested Circulation *(Sum of 10B1 and 10B2)*	3319	3531
D. Free Distribution by Mail, Carrier or Other Means Samples, Complimentary, and Other Free Copies	198	198
E. Total Distribution *(Sum of C and D)*	3517	3729
F. Copies Not Distributed 1. Office use, left over, unaccounted, spoiled after printing	233	171
2. Return from News Agents	---	---
G. TOTAL *(Sum of E, F1 and 2—should equal net press run shown in A)*	3750	3900

11. I certify that the statements made by — Signature and Title of Editor, Publisher, Business Manager, or Owner: Controller